LHC Run 2 and future prospects

J. T. Boyd
CERN, Geneva, Switzerland

Abstract
The lecture discusses both the current status of the Large Hadron Collider as well as its future running scenarios. In addition, a selection of the latest physics results from the experiments ATLAS, CMS and LHCb is presented.

Keywords
Particle accelerators, Particle physics, LHC Run 2; Lectures.

1 The Large Hadron Collider

The Large Hadron Collider (LHC) is the highest-energy particle collider in the world. The accelerator sits in a 27 km long tunnel, originally constructed for the Large Electron–Positron Collider (LEP), 100 metres underground at CERN, on the Franco-Swiss border near Geneva, Switzerland. It is an extremely sophisticated machine, using super conducting 8 T dipole magnets to steer the high-energy proton beams. The magnets are cooled to an operating temperature of 1.9 K by using superfluid liquid helium. Given the extreme energy of the beams, the LHC needs a complex machine protection system, relying on a large number of beam instrumentation devices to monitor the beam position and beam losses.

The two key parameters for a collider are the collision energy and the luminosity L, which is a measure of the number of collisions. The number of events for a specific process (N) is given by $N = \sigma \times L$, where σ is the production cross-section for that process and L is the integrated luminosity.

The luminosity at a collider is given by the formula: $L = n_{\mathrm{b}} N_1 N_2 F / 4\pi\epsilon\beta^*$ and can be increased by augmenting the number of protons per bunch (N_1, N_2), the number of colliding bunches (n_{b}), or reducing the transverse size of the beam at the collision point. This can be done by using a lower emittance (ϵ) beam, or by squeezing the beam more with the focusing magnets (reducing β^*). The crossing-angle between the beams, needed to avoid parasitic collisions due to the short distance between bunches, reduces the luminosity, and is encapsulated in the geometric factor F in the equation.

The main machine parameters for the LHC are shown in Table 1, for the design, Run 1, Run 2, as well as the expectation for Run 3 and the high-luminosity upgrade (HL-LHC). It can be seen that all of the design parameters have been exceeded, except the collision energy, and the number of colliding bunches. The LHC experts have continually improved the running scenario to increase the luminosity, and during Run 2 the design luminosity of 10^{34} cm^{-2}s^{-1}, was achieved and surpassed by a factor of two at the end of Run 2. As well as improving the instantaneous luminosity, the availability of the machine was dramatically improved from 2016 to 2018, which led to a large physics dataset. The machine provided collisions during 50% of the allocated physics time—a very impressive performance for a super conducting collider. An important parameter for the LHC experiments is the pileup, which is determined by the luminosity per bunch, and is a measure of the number of inelastic pp interactions that occur per bunch crossing. Higher pileup gives more luminosity (for a fixed number of bunches), but makes physics analysis more difficult due to the signals in the detector from the additional interactions.

Construction of the HL-LHC should be completed in 2026 and will be followed by at least ten years of operation, with the goal of reaching 3000 fb^{-1} in 2037 (an increase of a factor of ten compared to the expected dataset at that time). In order to achieve this, the injector needs to be upgraded to provide a higher intensity beam, the focusing magnets will be replaced to squeeze the beam further, and various components will be upgraded to cope with the increased radiation and stored energy. The pileup in ATLAS and CMS will increase significantly (to a maximum of 200 interactions per bunch crossing) and

the detectors will need large upgrades to be able to make physics measurements at this large pileup, as well as to cope with the associated radiation.

Table 1: Summary of main accelerator parameters for the LHC, showing the design values, and those used during Run 1 and Run 2, as well as the expected parameters for Run 3 and the HL-LHC.

Parameter	Design	Run 1	Run 2	Run 3	HL-LHC
Energy [TeV]	14	7/8	13	14	14
Bunch spacing [ns]	25	50	25	25	25
Bunch intensity [10^{11} ppb]	1.15	1.6	1.2	up to 1.8	2.2
Number of bunches	2800	1400	2500	2800	2800
Emittance [μm]	3.5	2.2	2.2	2.5	2.5
β^* [cm]	55	80	$30 \rightarrow 25$	$30 \rightarrow 25$	down to 15
Crossing angle [μrad]	285	-	$300 \rightarrow 260$	$300 \rightarrow 260$	TBD
Peak luminosity [10^{34} cm^{-2}s^{-1}]	1.0	0.8	2.0	2.0	7.5
Peak pileup	25	45	60	55	200

2 Run 2 physics highlights and future prospects

2.1 The LHC detectors

ATLAS and CMS are the general-purpose detectors at the LHC with the same physics goals. There are significant differences in the detector designs, but despite these they have very similar physics performance.

The main differences in the detectors relate to the magnet design. ATLAS is equipped with a 2 T solenoid to provide the magnetic field to bend charged particles in the central detector region, with three toroidal magnets (one barrel and two endcap toroid systems) to bend muons in the muon spectrometer. CMS uses a single large solenoid with field of 3.8 T for both of these roles. Following on from this, the ATLAS calorimeters are placed outside the thin solenoid, whereas the CMS calorimeters are placed inside the solenoid.

2.2 The Run 2 dataset

During the LHC Run 2 period, from 2015 to 2018, the ATLAS and CMS experiments collected, each of them, a sample of pp collisions at a center of mass energy of 13 TeV corresponding to an integrated luminosity of around 140 fb^{-1}. These large data samples could be collected thanks to the exceptionally good LHC operation efficiency and to instantaneous luminosities exceeding the design value (10^{34} cm^{-2}s^{-1}). The downside of running at such high instantaneous luminosities is that the interesting pp collision (the one that gives the trigger for the readout of the data) occurs together with many other pp collisions in the same bunch crossing, the so-called pileup. For example, the average pileup in the ATLAS experiment increased from around 13 collisions in 2015 to around 36 collisions in 2018, as shown in the left panel of Fig. 1, where we also see that some fraction of the collected events include almost 70 “extra" simultaneous pp collisions. To cope with the challenges induced by such large pileup values, the experiments developed improved procedures, at all levels, from the trigger to the offline data reconstruction and analysis. Examples of successful outcomes of those improvements are shown in the middle and right panels of Fig. 1.

2.3 Higgs physics

The main modes for Higgs production at the LHC are (in order of decreasing cross-section): gluon-fusion (ggF), vector-boson fusion (VBF), production in association with a vector boson (VH) and production in association with a pair of top-quarks (ttH). In VBF production, the scattered quarks are likely to form

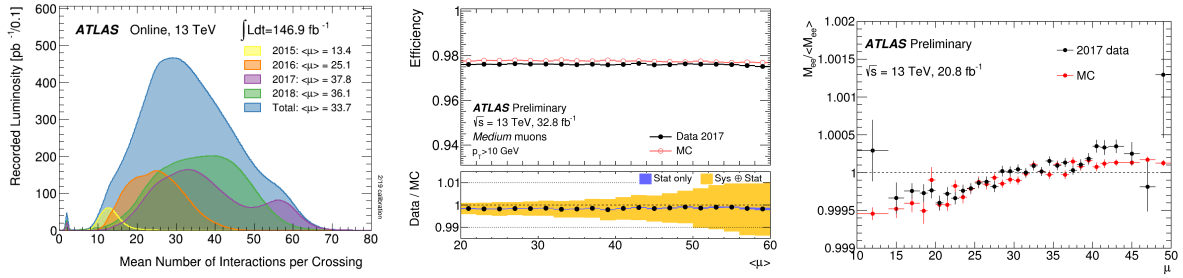

Fig. 1: (left) The Run 2 pileup distribution. An example of the pileup robustness of (middle) the reconstructed muon efficiency and (right) the electron energy scale.

forward jets on the two sides of the detector, which can be used to tag such events. The main decay modes for the Higgs boson are shown in Table 2. Experimentally the modes with the best mass resolution are important, as this allows to separate the signal from the background in a much more reliable way. The $H \to \gamma\gamma$ and $H \to ZZ^* \to 4\ell$ ($\ell = e/\mu$) have both excellent mass resolution of ≈1–2%. These were the modes used for the Higgs discovery in 2012, despite the fact they have very low branching fractions (BF). Figure 2 shows the mass distributions for these two channels for the full Run 2 dataset. For $H \to \gamma\gamma$ the signal to background (S/B) is low, but the total number of selected Higgs events is a few thousand, whereas for $H \to 4\ell$ the S/B is high. The total number of signal events is an order of magnitude less.

Table 2: Summary of Higgs decay modes (BFs and resolutions) for the 125 GeV mass SM Higgs boson. For the good mass resolution channels involving a Z-boson, the resolution is only good for leptonic decays of the Z.

Poor mass resolution channels		Good mass resolution channels	
Decay mode	BF (%)	Decay mode	BF (%)
$H \to b\bar{b}$	58.2	$H \to ZZ^*$	2.6 (0.012 e, μ)
$H \to WW^*$	21.4 (1.1 e, μ)	$H \to \gamma\gamma$	0.23
$H \to gg$	8.2	$H \to Z\gamma$	0.15 (0.008 e, μ)
$H \to \tau^+\tau^-$	6.3	$H \to \mu^+\mu^-$	0.02
$H \to c\bar{c}$	2.9		

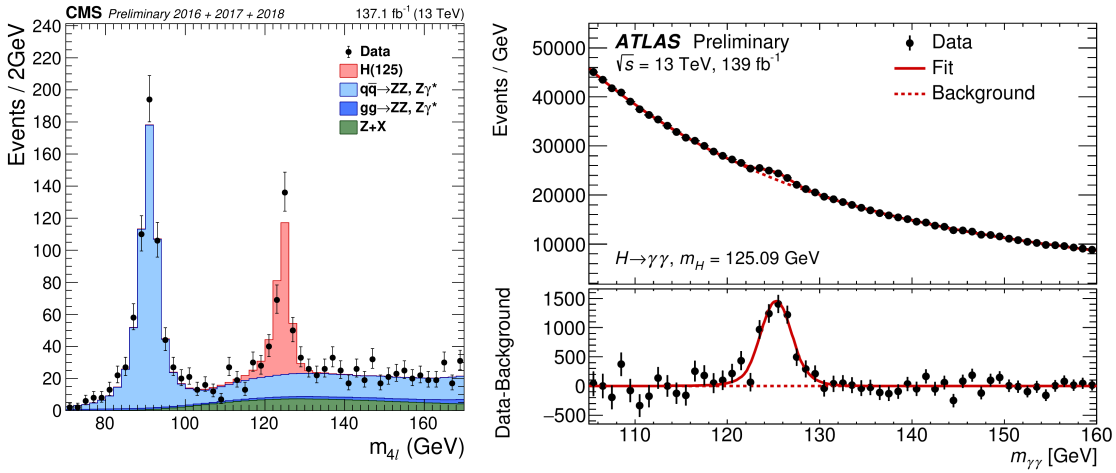

Fig. 2: Reconstructed Higgs candidate mass distributions in the $H \to \gamma\gamma$ (left) and $H \to 4\ell$ (right) channels.

Table 3 shows the status of the main Higgs production and decay modes, in terms of the signif-

icance of the measured signal. It shows that all of the main production and decay modes have been established, although many of these were only observed in the last year.

Table 3: Status of the measured significance for the main Higgs production and decay modes. Here Obs./Evid. means the significance is at the level of an observation/evidence, UL stands for 'upper limit' and '-' implies this mode has not been studied yet.

	$\gamma\gamma$	ZZ^*	WW^*	$b\bar{b}$	$c\bar{c}$	$\tau^+\tau^-$	$\mu^+\mu^-$	**Combined**
ggF	Obs.	Obs.	Obs.	-	-	UL	UL	Obs.
VBF	UL	UL	UL	UL	-	Evid.	UL	Obs.
VH	UL	UL	UL	Obs.	UL	-	-	Obs.
ttH	Evid.	UL	Evid.	UL	-	Evid.	-	Obs.
Combined	Obs.	Obs.	Obs.	Obs.	UL	Obs.	UL	-

The Higgs coupling to fermions was established with the observation of the $H \to \tau^+\tau^-$ decay. The analysis selects events with two τs (that either can decay hadronically or leptonically), and uses selections targeting either VBF Higgs production or high-p_{T} ggF Higgs production to reduce the backgrounds. The main background is $Z \to \tau^+\tau^-$ which has the same final state, with $\approx$1000$\times$ higher cross-section and with a similar di-τ mass (the mass resolution is not sufficient to be able to resolve the two processes). Figure 3 shows the di-τ mass distribution from the Run 2 CMS analysis [1] where a tiny signal can be seen on top of the large $Z \to \tau\tau$ background. The analysis measured the $H \to \tau\tau$ rate to be compatible with the SM expectation with a precision of $\approx$30%, corresponding to a 5.9 σ observation of the process. Searches for $H \to \mu^+\mu^-$ have found no evidence of a signal (as expected in the SM for the current dataset), which when combined with the $H \to \tau^+\tau^-$ result, demonstrates that the Higgs couplings do not obey lepton flavour conservation.

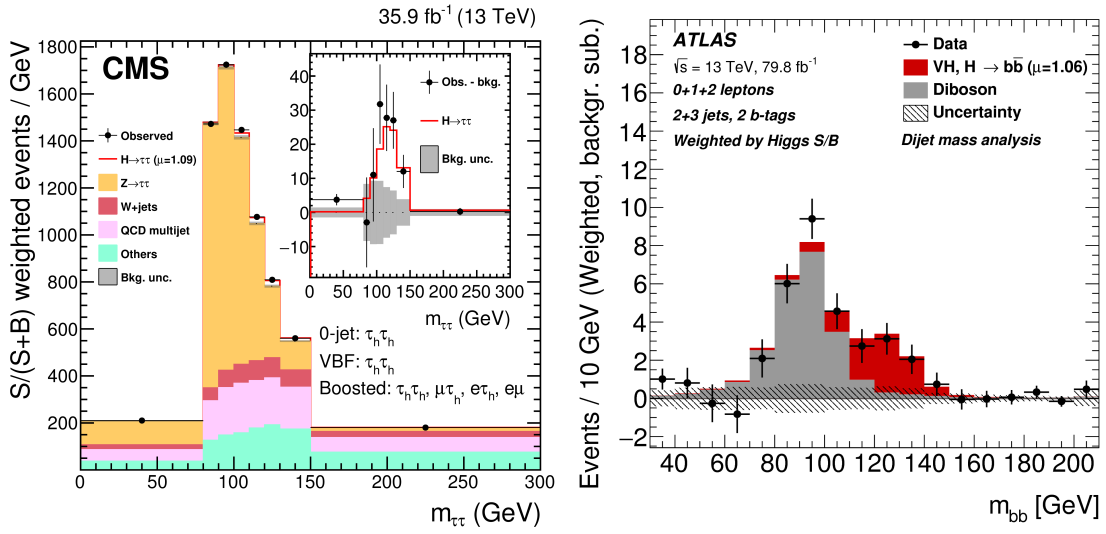

Fig. 3: (left) The di-tau mass distribution from the CMS $H \to \tau^+\tau^-$ analysis; (right) The di-b-jet mass distribution from the ATLAS $H \to b\bar{b}$ analysis.

The Higgs coupling to quarks was established with the observation of $H \to b\bar{b}$. Although this has the largest Higgs decay BF, it is experimentally challenging due to the large background from QCD $b\bar{b}$ production, and the poor di-b-jet mass resolution. In order to reduce the background and to trigger on the events, the analysis targets VH production where V is a Z or W boson decaying leptonically, so the final state can have 2 leptons, 1 lepton or 0 leptons (but large missing transverse momentum (MET) from the $Z \to \nu\bar{\nu}$ decay), and selects two b-jets with a mass close to the Higgs mass. As seen in Fig. 3, which

shows the ATLAS analysis [2], the VZ, $Z \to b\bar{b}$ decay acts as an important validation of the analysis. This has the same final state, with a similar rate. The figure shows that VZ is observed with the expected rate (grey), and the $H \to b\bar{b}$ signal can be seen as a high mass shoulder on the Z peak. The analysis finds the expected SM rate with a precision of ≈30%.

The Higgs is too light to decay to top quarks, so the top-Higgs (tH) coupling can only be directly probed through ttH production. In the SM the ggF production process is dominated by a top-quark in the ggF loop, and so the tH coupling can also be extracted indirectly from ggF production rates. The direct and indirect measurement of the coupling then allow to constrain possible new-particles that could enter the ggF loop. Within the current precision the direct and indirect measurements of the coupling are compatible.

With the increased luminosity at the HL-LHC, the Higgs physics goals are:

- Improve the precision on the Higgs couplings to the few-% level (where they can be sensitive to effects beyond the SM (BSM);
- Establish the coupling to 2nd generation fermions through the $H \to \mu^+\mu^-$ and $H \to c\bar{c}$ decays;
- Improve the constraints on forbidden Higgs decays such as $H \to$ invisible and lepton-flavour violating Higgs decays;
- Make more precise differential measurements of Higgs production in more extreme regions of phase-space, which could be sensitive to new physics;
- Observe the very rare di-Higgs production process.

Studying di-Higgs production is needed to understand the Higgs self-coupling, and to probe the Higgs potential term of the SM Lagrangian. However, it is doubtful that this will be possible at the HL-LHC. Current projections [3, 4] suggest that evidence for di-Higgs production can be achieved by combining the ATLAS and CMS HL-LHC results.

2.4 Searches for physics beyond the Standard Model

One of the primary goals of the LHC is to search for the direct production of BSM physics. ATLAS and CMS have carried out a huge number of searches, but to date no significant excess of events over the SM expectation has been observed. A few example searches are discussed below.

A search for a new gauge boson (Z') that is similar to the SM Z boson but with much higher mass, looks for an excess of events in the di-lepton mass spectra at high mass. Figure 4 shows the di-electron and di-muon mass distributions from the ATLAS search [5]. No significant deviation from the expected background (dominated by SM Drell-Yan production) is observed. Examples signals are shown in the figures, which show that the mass resolution is significantly better at high mass for electrons than for muons, as the energy resolution improves for calorimeters, but deteriorates for tracking detectors, at higher energy. The main experimental challenge for this search is to have good efficiency and resolution for very high transverse momentum leptons (up to 2 TeV).

At the other end of the spectrum is a search for Higgsino production where very low-momentum leptons are expected. The ATLAS search [6] uses leptons with p_{T} down to 3 GeV (muons) and 4.5 GeV (electrons) in order to improve the sensitivity, and allows to exclude Higgsinos with masses up to 150 GeV for certain mass splittings.

Searching for dark matter (DM) production in LHC collisions can be done by taking advantage of initial-state-radiation, which can be used to tag events where DM particles are pair produced through an s-channel mediator particle but escape the detector without interacting with it. This can lead to a detector signature of a high-p_{T} jet + MET. Figure 5 shows the MET spectrum for such events from the CMS search [7], also showing the expected background, dominated by $Z \to \nu\bar{\nu}$ + jets (≈60%) and $W \to \ell\nu$ + jets (where the lepton is not reconstructed) (≈30%). The signal has a slightly harder MET-spectra than the background, but is much smaller than the background, meaning the background needs

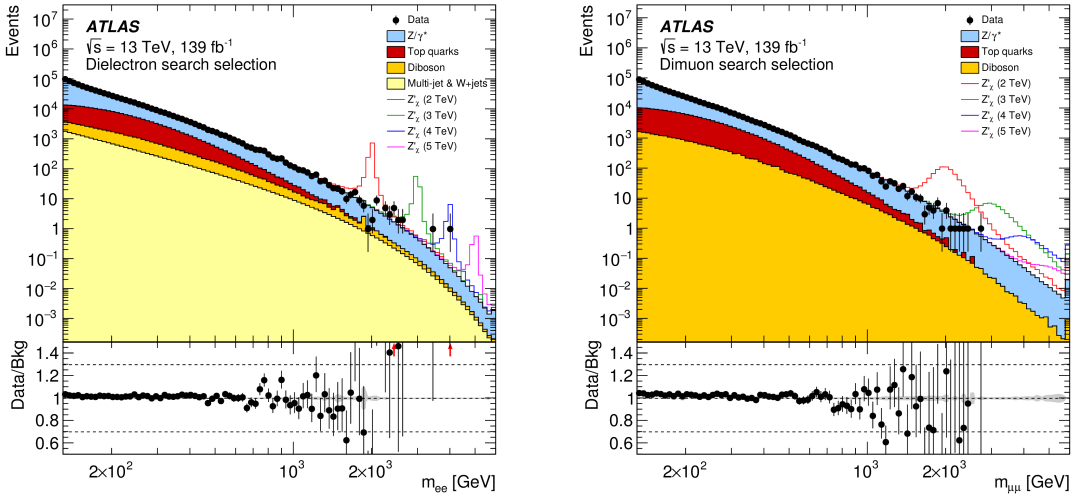

Fig. 4: The di-electron and di-muon mass distributions from the ATLAS Z' search.

to be controlled at the few-% level to allow to have sensitivity. The background is estimated from data control regions with $Z \to \ell^+\ell^-$ + jets, $W \to \ell\nu$ + jets and γ + jets but accurate theoretical predictions are needed on the ratio of Z + jets/γ + jets and Z + jets/W + jets; in order to achieve the needed precision NNLO electroweak corrections need to be taken into account.

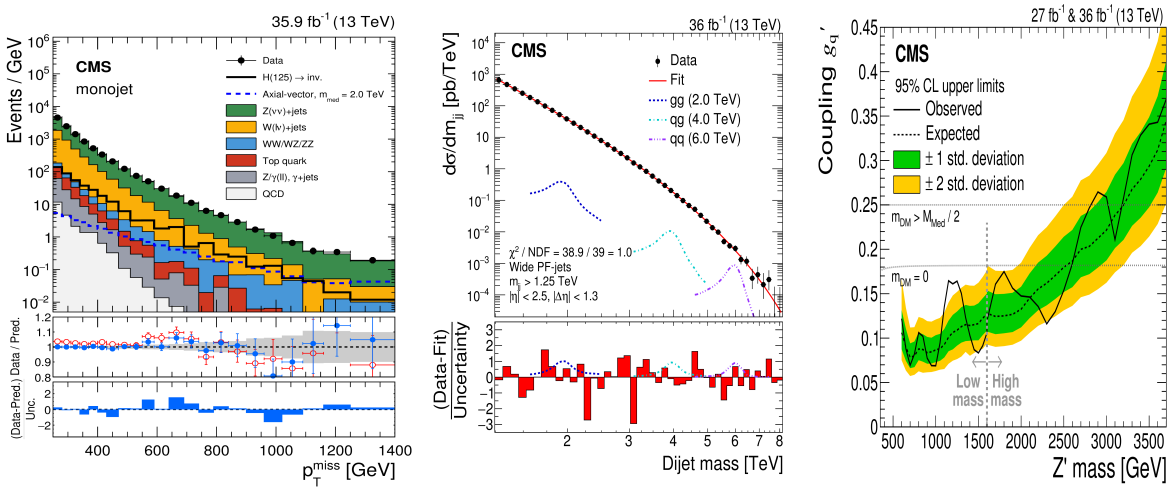

Fig. 5: (left) The MET spectrum in the DM search; (middle) The di-jet mass spectra in the mediator search; (right) The exclusion limit in the search for the mediator showing results for both the high mass search, and the low mass search that uses the *Data Scouting* technique.

As well as searching for the DM particle, we can also search for a mediator that can be produced in the LHC collisions, but decays back to SM particles (for example to two quarks). This could show up as a resonance in the di-jet mass spectra. Figure 5 shows the di-jet mass distribution for such a CMS search [8], showing a smoothly falling distribution with no sign of a resonance in the range 1 TeV to 8 TeV in the di-jet mass. The 1 TeV lower limit in the probed mass range comes from the trigger thresholds applied to the jets used in the search. Going to lower p_{T}-jets would increase the trigger rate leading to a too high bandwidth when reading out the detector. In order to search for possible resonances at lower mass a new technique called *Data Scouting* or *Trigger Level Analysis* was developed, in which

just the trigger level jets are written out for certain triggers. These trigger level jets are much smaller than the full event data (less than 5% of the size), and can therefore be read out at a much higher rate without hitting bandwidth limitations. Thus lower thresholds can be applied. This technique allows for setting limits on di-jet mass resonances down to lower masses, as can be seen in Fig. 5 (CMS analysis [8]).

2.5 Precise Standard Model measurements

The LHC experiments carry out a large number of precise measurements of SM processes, measuring cross-sections, masses and other SM parameters. Cross-section measurements are normalized by the luminosity, which is measured by dedicated luminosity detectors in the experiments that are calibrated by dedicated van-der-Meer scans that are typically carried out each year. The precision of the luminosity measurements in ATLAS and CMS for the Run 2 dataset is an impressive ≈2.5%, which is far better than had thought to be possible before LHC running.

An example of a very precise cross-section measurement is the W and Z inclusive production cross-section measurement from ATLAS [9] with the 2011 7 TeV dataset. The precision is limited by systematic uncertainties, and the total experimental uncertainty is ≈0.5% dominated by uncertainties related to the lepton reconstruction, the background (for the W) and theoretical modeling uncertainties (for the Z). The luminosity uncertainty is 1.8%, but this cancels in ratios such as $\sigma(W \to e\nu)/\sigma(W \to \mu\nu)$ or $\sigma(W)/\sigma(Z)$ allowing very precise tests of lepton flavour conservation, and parton distribution functions (PDFs).

The measurement of the W-boson mass by ATLAS [10], with a precision of 19 MeV, represents one of the most precise measurements at the LHC and has a precision equal to the best single-experiment measurement. The W-mass is a fundamental parameter of the SM, and has important sensitivity in the electroweak fit. The ATLAS analysis measures the mass using a template, which fits to the transverse mass (formed from the lepton and the reconstructed hadronic recoil) and to the lepton transverse momentum. A very precise knowledge of experimental effects related to lepton reconstruction and the hadronic recoil reconstruction is needed, where the later deteriorates significantly with pileup. The current measurement utilizes the 2011 7 TeV data set which has an average pileup of around 9. Theoretical uncertainties also play an important role, in particular related to the modelling of the W-boson p_{T} which is derived from the measured Z-boson p_{T} spectra, as well as from Parton Distribution Function (PDF) uncertainties. Utilizing low-pileup data taken in 2017 and 2018 at 13 TeV there is the prospect of improving the precision of the measurement to the 10–15 MeV level.

Measurements of the top-quark mass are carried out in a number of different channels. A recent example from CMS [11] utilizes the lepton + jets final state to measure the mass using a kinematic fit (including the W-mass constraint on the hadronic W decay) to improve the resolution and to reduce the fraction of incorrect assignments of jets to the two top-quarks. The dominant systematic uncertainty is related to the jet energy scale which is constrained in the fit. The final result of $172.25 \pm 0.08(\mathrm{stat.}) \pm 0.62(\mathrm{syst.})$ GeV is the most precise single measurement to date.

2.6 Flavour physics

The $B_S \to \mu^+\mu^-$ rare decay is theoretically clean, and has a large sensitivity to many new physics models (for example MSSM scenarios with large tan β). Because of this, there is a long history of searches for this decay that started over 30 years ago. Sensitivity to the SM branching ratio of $(3.3 \pm 0.3) \times 10^{-9}$ was reached with a combination between LHCb and CMS [12]. Despite a much smaller dataset, LHCb has the best sensitivity due to the excellent track resolution, as well as an optimized trigger for low p_{T} physics; CMS has better sensitivity than ATLAS, due to the higher magnetic field in the inner tracker, which gives a better mass resolution. Current measurements from all three experiments are consistent with the SM estimate with an uncertainty from 20 to 30%.

LHCb searches for lepton flavour violation in B meson decays by measuring the ratio $R_{K^{(*)}} \equiv$

$\mathrm{BF}(B \to K^{(*)}\mu^+\mu^-)/\mathrm{BF}(B \to K^{(*)}e^+e^-)$. In the SM this is precisely predicted and is close to unity, modulo phase-space effects. Bremsstrahlung represents an experimental complication as the mass resolution is much worse in the di-electron channel than in the di-muon channel (as can be seen in Fig. 6). This is corrected for by normalizing by the measured ratio $\mathrm{BF}(B \to K^{(*)}J/\psi(\mu^+\mu^-))$ / $\mathrm{BF}(B \to K^{(*)}J/\psi(e^+e^-))$. For R_K, the reconstructed B meson mass distribution is shown in Fig. 6 in both the $\mu^+\mu^-$ and e^+e^- channels. The measured values from the LHCb measurements [13, 14] are shown in Table 4, and for R_{K^*} in Fig. 6. It is shown that the three measurements are between 2 and 2.5 σ lower than the SM prediction. This is currently one of the most intriguing anomalies observed by the LHC experiments, with many theoretical models proposed to explain the results. More data and measurements from Belle-2 should shed further light onto the situation.

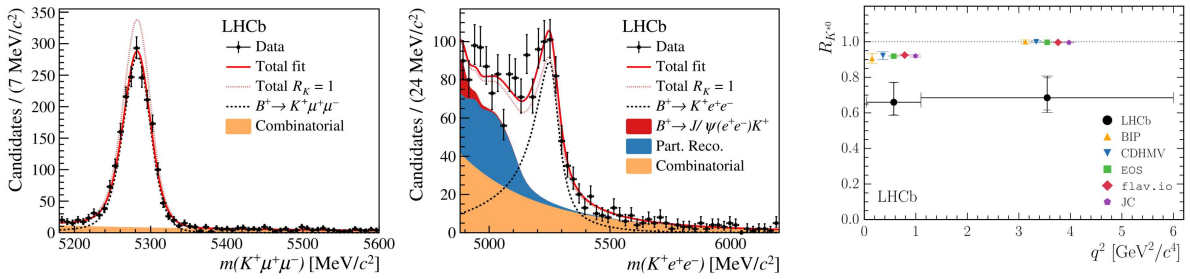

Fig. 6: Left/middle: The reconstructed B meson mass in the R_K analysis for the $\mu^+\mu^-$ / e^+e^- channels; Right: The measured R_{K^*} values in two bins of q^2 (the di-lepton mass) compared with various theoretical predictions.

Table 4: LHCb results on lepton flavour violation measurements R_K and R_{K^*}, where the latter is measured in two regions of q^2 (the di-lepton mass).

Measurement	Dataset	Measured value	Compatibility with SM
R_K	Run 1 + Run 2	$0.85^{+0.06}_{-0.05} \pm 0.015$	2.5σ
R_{K^*} low-q^2	Run 1	$0.66^{+0.11}_{-0.07} \pm 0.03$	2.2σ
R_{K^*} high-q^2	Run 1	$0.69^{+0.11}_{-0.07} \pm 0.05$	2.4σ

3 Summary

The LHC machine and the experiments performed extremely well in Run 2. A large and high-quality dataset was produced by the experiments leading to a huge number of physics results. A leading challenge for the experiments was the high pileup in the data, but they have coped very well with this situation.

The large dataset has allowed a more and more precise probing of the Higgs boson, where all major production modes and decay channels accessible at the LHC have been established. A huge number of direct searches for BSM physics have been carried out, with no significant excess of events over the SM prediction observed, such that increasingly stringent exclusion limits have been set on BSM model parameters. In addition, the experiments have been able to make very precise measurements of cross-sections and SM parameters, as well as measuring extremely rare processes, but again no discrepancy with the SM expectations have been observed. An intriguing set of results from lepton-flavour violation measurements by LHCb show a 2–2.5 standard deviation discrepancy with the SM in a few channels and q^2-bins.

The increased dataset that will be produced with Run 3, and then with the HL-LHC, along with the upgraded detector functionality, and innovations in triggering, reconstruction and physics analysis will

allow to probe further the SM in the coming years.

References

[1] A.M. Sirunyan *et al.* [CMS Collaboration], *Phys. Lett.* **B779** (2018) 283–316, doi:10.1016/j.physletb.2018.02.004.

[2] M. Aaboud *et al.* [ATLAS Collaboration], *Phys. Lett.* **B786** (2018) 59–86, doi:10.1016/j.physletb.2018.09.013.

[3] CMS Collaboration, Sensitivity projections for Higgs boson properties measurements at the HL-LHC, CMS-PAS-FTR-18-011 (2018), https://cds.cern.ch/record/2647699.

[4] ATLAS Collaboration, Projections for measurements of Higgs boson cross sections, branching ratios, coupling parameters and mass with the ATLAS detector at the HL-LHC, ATL-PHYS-PUB-2018-054 (2018), http://cdsweb.cern.ch/record/2652762.

[5] G. Aad *et al.* [ATLAS Collaboration], *Phys. Lett.* **B796** (2019) 68–87, doi:10.1016/j.physletb.2019.07.016.

[6] G. Aad *et al.* [ATLAS Collaboration], *Phys. Rev.* **D101** (2020) 052005, doi:10.1103/PhysRevD.101.052005.

[7] A.M. Sirunyan *et al.* [CMS Collaboration], *Phys. Rev.* **D97** (2018) 092005, doi:10.1103/PhysRevD.97.092005.

[8] A.M. Sirunyan *et al.* [CMS Collaboration], *JHEP* **08** (2018) 130, doi:10.1007/JHEP08(2018)130.

[9] M. Aaboud *et al.* [ATLAS Collaboration], *Eur. Phys. J.* **C77** (2017) 367, doi:10.1140/epjc/s10052-017-4911-9.

[10] M. Aaboud *et al.* [ATLAS Collaboration], *Eur. Phys. J.* **C78** (2018) 110, doi:10.1140/epjc/s10052-017-5475-4
Erratum: *Eur. Phys. J.* **C78** (2018) 898, doi:10.1140/epjc/s10052-018-6354-3.

[11] A.M. Sirunyan *et al.* [CMS Collaboration], *Eur. Phys. J.* **C78** (2018) 891, doi:10.1140/epjc/s10052-018-6332-9.

[12] V. Khachatryan *et al.* [CMS and LHCb Collaborations], *Nature* **522** (2015) 68–72, doi:10.1038/nature14474.

[13] R. Aaij *et al.* [LHCb Collaboration], *JHEP* **08** (2017) 055, doi:10.1007/JHEP08(2017)055.

[14] R. Aaij *et al.* [LHCb Collaboration], *Phys. Rev. Lett.* **122** (2019) 191801, doi:10.1103/PhysRevLett.122.191801.